Ibn Al-Haitham Journal for Pure and Applied Sciences
Journal homepage: jih.uobaghdad.edu.iq
PISSN: 1609-4042, EISSN: 2521-3407
IHJPAS. 2025, 38(2)

Synthesis, Characterization, and Study of Liquid Crystals Properties of New Five Heterocyclic Compounds

Adiba K. Amine[1] and **Nisreen H. Karam**[2*]
[1,2]Department of Chemistry, College of Education for Pure Science (Ibn Al-Haitham), University of Baghdad, Baghdad, Iraq.
*Corresponding Author.

Received: 21 March 2023 Accepted: 8 October 2023 Published: 20 April 2025
doi.org/10.30526/38.2.3354

Abstract

Heterocyclic compounds are employed in many applications, and numerous researchers have created liquid crystals by adding heterocyclic to the structures of these molecules. This work includes the synthesis and characterization of new compounds that contain 5H-thiazolo [4,3-b][1,3,4] thiadiazol united in multiple steps, starting with the synthesis of the aldehyde compound [I] by reaction chloro ethyl acetate with 4-hydroxybenzaldehyde in the presence of ethanol and potassium carbonate, followed by reactions with thiosemicarbazide, mercapto acetic acid in sulphuric acid to produce compound [II] then reflux compound [II] with hydrazine hydrate to product compound [III], after that reaction the later compound with n-alkoxybenzaldehyde $[IV]_n$ and a few drops of piperidine in THF as a solvent to produce new Schiff's-bases compounds contain 5H-thiazolo [4,3-b] [1,3,4] thiadiazol unite [V]n, FTIR and ^{1}HNMR spectroscopy were used to analyze the compounds, a polarized optical microscope (POM) and differential scanning calorimetry (DSC) were used to examine the characteristics of the liquid crystals. In the Smectic A (SmA) and nematic phases, liquid crystal characteristics are present in all compounds [V]n. In addition to the nematic phase, all compounds $[V]_n$ showed enantiotropic dimorphism in the SmA phase. It was revealed that compounds $[V]_n$ with 5H- thiazole [4,3-b] [1,3,4]thiadiazol unit, the rigid-rod core of Schiff bases, and the formation of a supramolecular hydrogen bond between the derivatives $[V]_n$ had liquid crystallinity, depending on the chain length of the alkoxy group as a terminal substituent.

Keywords: Heterocyclics, Isotropic, Liquid crystal, Mesomorphic, Thiazolo[4,3-b][1,3,4] thiadiazol.

1. Introduction

Between the characteristics of traditional liquids and those of solid crystals, liquid crystals are substances in a state (1). Because heterocyclic compounds are employed in many applications, numerous researchers created liquid crystals by adding heterocyclic to the structures of these molecules (2-6). It is common knowledge that the molecular structure of organic materials plays a significant role in determining their physical properties. When creating the material for the gadget, looking at the structure-activity interactions is helpful in applications (3-5). They also have excellent optical qualities essential for displays and other state readouts. Recently, liquid crystals have been utilized as a model system that responds to the environment's molecular makeup (6-10). The importance of compounds with heterocyclic ring structures cannot be overstated.

Both for medical and commercial purposes, in the last two decades, the use of five-member heterocyclic rings as molecular building blocks has received a lot of interest (11). Recent advances were evaluated and summarized to prepare other thiadiazoles. Subclasses of fused 5H-thiazolo[4,3-b]-the relative configurations of sulfur and nitrogen atoms and numerous sites for fusion between the thiazole and thiadiazole rings form 1,3,4-thiadiazoles (12-21). This work aims to synthesize, characterize the structure, and investigate the liquid crystal behavior for compounds containing the 5H-thiazolo[4,3-b][1,3,4]thiadiazol ring as part of a current investigation of liquid crystal derivatives containing heterocyclic units. Also, this study aims to investigate the influence of heterocyclics on the behavior of liquid crystals.

2. Materials and Methods

The materials were taken from Aldrich, Fluka, and Merck Co. The ^{1}H-NMR spectra were measured by Bruker company at 400 MHz and were reported in ppm(δ); the compounds were dissolved in DMSO-d6 solution with the TMS as the internal standard. FTIR spectra were recorded by SHIMADZU(IR Affinity-1) FTIR spectrometer in the wave number range 4000-600 cm^{-1}; The Gallen Kamp apparatus's melting point measurement. The polarized optical microscope (POM) model Leica DM2500 M was used to examine the mesophase textures. In **Scheme 1**, the path taken to create new compounds is depicted. The samples were analyzed using cross polarizers at normal temperature with a magnification of 10 and elevated temperature with a magnification of 20. The temperature was raised initially quickly at 5 °C/min. At the University of Tehran, differential scanning calorimetry (DSC) measurements were taken using a German-made device using the Q600 and 5 ⁰C/minute.

2.1. Synthesis of 1-((2-ethoxyallyl)oxy)-4-vinylbenzene [I]

Potassium carbonate (1.31 g, 0.001 mol) was added in ethanol with 4-hydroxybenzaldehyde (0.85 g, 0.001 mol), ethyl chloroacetate (0.12 g, 0.001 mol), and (5 mL). The mixture was refluxed for 6 hours. After being added, the ethyl acetate was removed from the organic layer, dried, and then crystallized again from ethanol. 97% of the yellow color's molecular formula, $C_{11}H_{12}O_4$, is produced as oil.

FTIR (cm^{-1}): 1755 for C=O ester, 1689 for C=O aldehyde, and 1600 for C=C. (ppm) ^{1}HNMR(400 MHZ,DMSO-d$_6$): 1.06-1.24 (t,3H,CH_3), 4.11-4.88 (q,2H, OCH_2CH_3), 4.94 (s,2H, OCH_2), 6.71-7.93 (m,4H, Ar-H), 9.89 (s,1H,CHO).

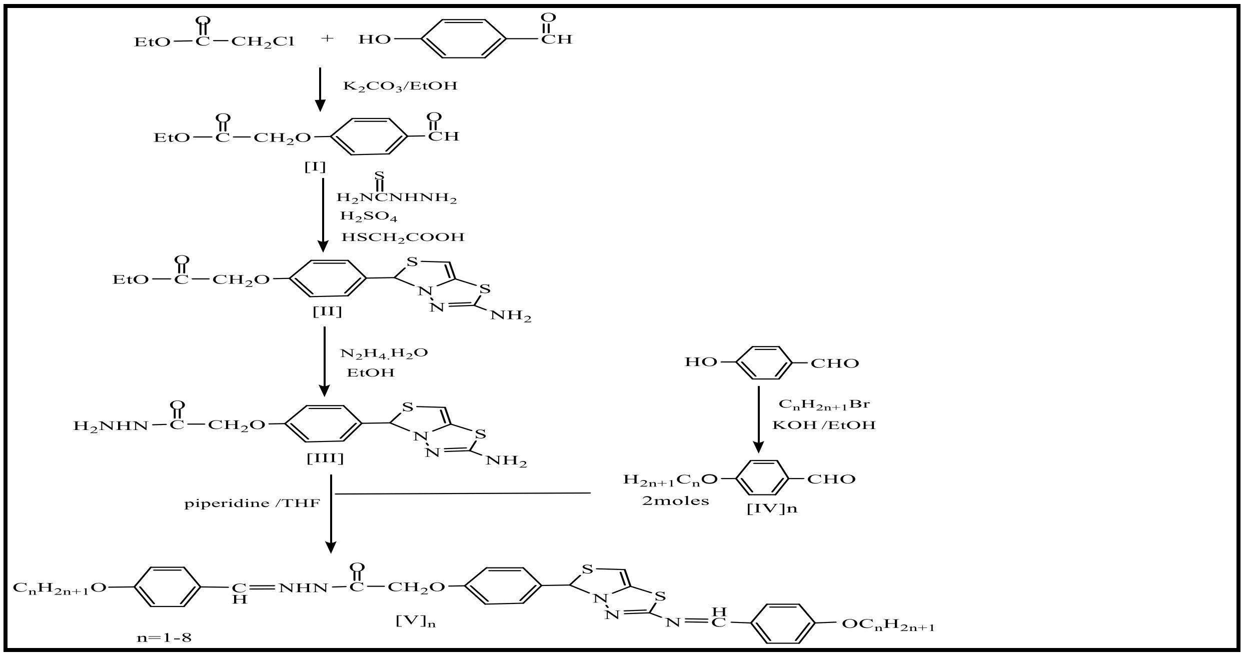

Scheme 1. Route of synthesis compounds [I]-[V]8.

2.2. Synthesis of ethyl 2-(4-(2-amino-5H-thiazolo[4,3-b][1,3,4]thiadiazol-5-yl)phenoxy) acetate [II]

Mercapto acetic acid (0.92 g, 0.01 mol) and compound [I] (2.08 g, 0.01 mol) were combined for 20–25 minutes. Thiosemicarbazide (0.91 g, 0.01 mol) was added, and concentrated sulfuric acid (7.5 mL) was added in portions after cooling. The mixture was placed in a freezer at 20 °C for 24 hours. The pH was then adjusted to 7-8 using 20 g of crushed ice and 40% aqueous sodium hydroxide (NaOH). The precipitate was dried and filtered (22); color: dark yellow; yield: 77%; m.p: > 300°C.

FTIR(cm^{-1}): 3302,3167(NH$_2$),1735(C=O ester),1620(C=N),1593(C=C).

1.09-1.22 (t, 3H, CH$_3$), 3.43-3.75 (q, 2H, $O\underline{CH_2}CH_3$), 3.77 (s, 2H, OCH$_2$), 3.93 (s, 2H,NH$_2$), 4.83 (s, H, (S-CH-N) in cyclic), 4.20 (s, H, (S-CH=C) in cyclic), 6.85-8.12 (ppm) for ^{1}H NMR at 400 MHz in (m,4H,Ar-H).

2.3. Synthesis of 2-(4-(2-amino-5H-thiazolo[4,3-b][1,3,4]thiadiazol-5-yl)phenoxy)-1-(1λ5-diazenyl) ethan-1-one [III]

Ester compound [II] (20.22 g, 0.006 mol) and hydrazine hydrate (1.5 mL) were combined and refluxed for 3 hours in absolute ethanol. After the mixture reached room temperature, the solvent was expelled, and the product (23), which had a melting point greater than 300°C and had a yellowish-green hue, was produced.

FTIR (cm^{-1}): 3429-3183 (NH,NH$_2$), 1678 (NHC=O), 1627 (C=N), and 1616 (C=C). ^{1}H NMR (400MHz, DMSO-d$_6$) (ppm): 3.60 (s, 2 H, OCH$_2$), 3.77 (s, 2 H, $NH\underline{NH_2}$), 3.84 (s, 2 H, NH$_2$), 4.57 (s, H, (S-CH-N) in cyclic), 4.53 (s, H, (S-CH=C) in cyclic), 6.88-8.10 (m, 4 H, Ar-H), and 8.32 (s, 1 H, NHC=O)

2.4. Preparation of 4-n-alkoxybenzaldehyde [IV]$_n$

In 50 mL of pure ethanol, 4 hydroxybenzaldehydes (10.61 g, 0.87 mol), n-alkyl bromide (0.13 mol), and potassium hydroxide (4.87 g, 0.87 mol) were dissolved. The mixture was refluxed for 6 hours, and potassium bromide was precipitated before 50 mL of water and 50 mL of ethyl ether were added. The organic phase of the combination was then taken out and rinsed with 25 mL of water, 25 mL of NaOH solution, and 25 mL of water. To get oily 4-alkoxybenzaldehyde, the organic phase was dried over magnesium sulfate, filtered, and evaporated.

2.5. Synthesis of Schiff-base compounds $[V]_n$

The 4-alkoxybenzaldehyde [IV]n (0.042 mol) and compound [III] (13.5 g, 0.042 mmol) were combined and refluxed for 4 hours in the presence of 3–4 drops of piperidine in THF (40 mL) (in a water bath). After evaporating the solvent, ethyl acetate was used to extract the residue.

^{1}HNMR (400MHz, DMSO-d6): 1.58(s, 3H, OCH_3), 3.74(s, 2H, OCH_2), 4.19(s, H, (S-CH=C) in cyclic), 6.91-7.84(m, 12H, Ar-H), 7.86(s, 2H, 2C=NH) and 8.63(s, 2H, 2C=NH) (s,1H,NH).

N'-(4-(ethyloxy) benzylidene)-2-(4-(2-((4-(ethyloxy) benzylidene) amino)-5*H*-thiazolo [4,3-b] Thiadiazol-5-yl) phenoxy) acetohydrazide [1,3,4] $[V]_2$, hue brown, yield 73%, melting point 160°C, FTIR (cm^{-1}): 3321 (NH), 2962 (CH aliph.), 1678(CONH), 1620 (C=N), and 1600 (C=C).

N'-(4-(propoxy) benzylidene) -2-(4-(2-((4-(propoxy) benzylidene) amino) -5*H*-thiazolo [4,3-b] [1,3,4] thiadiazol-5-yl) phenoxy)acetohydrazide $[V]_3$ yellow in hue, 70% yield, m.p. 170 ^oC, FTIR (cm^{-1}): 3363 (NH), 2962,2873 (CH aliph.), 1685 (CONH), 1624 (C=N), and 1600 (C=C). ^{1}HNMR (400MHz, DMSO-d6) (ppm): 1.03-1.07 (t, 6H, $2CH_3$), 1.81-1.83 (m, 4H, $2OCH_2CH_2$), 3.46 (t, 4H, $2OCH_2CH_2$), 4.05(s, 2H, OCH_2), 4.08(s, H, (S-CH-N) in cyclic), 4.07(s, H, (S-CH=C (s, 1H, NH).

N'-(4-(butyloxy) benzylidene)-2-(4-(2-((4-(butyloxy) benzylidene) amino)-5*H*-thiazolo [4,3-b] Thiadiazol-5-yl) phenoxy) acetohydrazide [1,3,4] $[V]_4$, hue brown, yield 97%, m.p. 165°C, and FTIR (cm^{-1}): 3100 (NH), 2962, 2870 (CH aliph.), 1678 (CONH), 1610 (C=N), and 1600 (C=C).

N'-(4-(pentyloxy) benzylidene)-2-(4-(2-((4-(pentyloxy) benzylidene) amino)-5*H*-thiazolo [4,3-b] [1,3,4] thiadiazol-5-yl) phenoxy)acetohydrazide $[V]_5$, brown, 74% yield, and gummy FTIR (cm^{-1}) values include 3210 (NH), 2974, 2860 (CH aliph.), 1689 (CONH), 1650 (C=N) and 1608 (C=C).

N'-(4-(hexyloxy) benzylidene)-2-(4-(2-((4-(hexyloxy) benzylidene) amino)-5*H*-thiazolo [4,3-b] [1,3,4] thiadiazol-5-yl)phenoxy)acetohydrazide $[V]_6$ is a brown substance with a 93% yield and gummy characteristics. FTIR (cm^{-1}) values include 3200 (NH), 2900, 2850 (CH aliph.), 1680 (CONH), 1630 (C=N) and 1600 (C=C).

N'-(4-(heptyloxy) benzylidene) -2-(4-(2-((4-(heptyloxy) benzylidene)amino)-5*H*-thiazolo[4,3-b] [1,3,4] thiadiazol-5-yl)phenoxy)acetohydrazide $[V]_7$, light brown; yield: 80%; melting point: 140 ^oC; FTIR (cm^{-1}): 3200 (NH); 2927; 2870; 1651; CONH; 1615; 1597 (C=C). ^{1}HNMR (400MHz, DMSO-d_6) ppm values include: 0.92-0.96 (t, 6H, $2CH_3$), 1.30-1.55 (m, 20H, $2OCH_2(CH_2)5CH_3$), 160-1.80 (t, 4H, $2OCH_2(CH_2)5CH_3$), 3.38 (s, 2H, OCH_2), 4.04 (s, H, (S-CH-N) & H, (S-CH= (s, 1H, NH).

N'-(4-(octyloxy) benzylidene)-2-(4-(2-((4-(octyloxy) benzylidene) amino)-5*H*-thiazolo [4,3-b] [1,3,4] thiadiazol-5-yl) phenoxy) acetohydrazide $[V]_8$, brown in color, yielding 71%, melting point 130 ^oC, with FTIR (cm^{-1}) readings of 3282(NH), 2924, 2850 (CH aliph.), 1670(CONH), 1630 (C=N) and 1604(C=C).

3. Results and Discussion

New compounds with the 5H-thiazolo[4,3-b][1,3,4] thiadiazol unite were subsequently synthesized and described. The observed FTIR and ^{1}HNMR spectroscopy values of the produced compounds matched the corresponding compounds' structures. Starting with 4-hydroxybenzaldehyde, ethyl chloroacetate and the presence of potassium carbonate in 100% ethanol are used to treat it to create 1-(2-ethoxyallyl) oxy)-4-vinylbenzene [I]. The stretching bands for carbonyl C=O for the ester group at (1755 cm^{-1}) (24) and carbonyl C=O for the aldehyde group at (1689 cm^{-1}) were visible in the FTIR spectra of compound [I]. The triplet and quartet signals in the ^{1}HNMR spectrum peaked at 1.06 and 1.24 ppm, (4.1 and 4.88 ppm), and 9.89 ppm, respectively, due to the CH_3 and OCH_2 of ester proton and aldehydic proton.

The compound [I] was reacted with thiosemicarbazide and mercaptoacetic acid in sulphonic acid to produce compound [II]. The FTIR spectrum showed the disappearance of absorption bands of the aldehyde group and the appearance of new characteristic bands at 3302, 3167 cm^{-1}, and 1620 cm^{-1}, which belong to the NH_2 and C=N groups, respectively. The ^{1}HNMR spectrum showed a peak at (1.19-1.22)ppm, δ(3.43-3.75) ppm as triplet and quartet signals at δ 3.93, 4.83,4.20 ppm of protons of NH_2,(s, H, (S-CH-N) and (s, H, (S-CH=C) in cyclic groups, respectively.By heating compound [II] with hydrazine hydrate at reflux, compound [III] was created. The FTIR spectrum demonstrated the elimination of ester group absorption bands. It revealed the emergence of new distinctive bands for the amide group at 1678 cm^{-1} C=O and bands for the NH and NH_2 groups at 3429 and 3182 cm^{-1}. The CONH proton and protons of (s, H, (S-CH-N), (s, H, (S-CH=C) in cyclic protons at 4.57,4.53 ppm in the ^{1}H NMR spectrum, respectively, are responsible for the peak at 8.32 ppm as a singlet. In the end, compound [III] reacted with n-alkoxybenzaldehyde $[IV]_n$ and a few drops of piperidine in THF to produce Schiff-bases compounds $[V]_n$. In the FTIR spectra of these Schiff base derivatives $[V]_n$, the band related to the NH_2 groups in compound [III] was absent, and in its place were bands in the range of 1610–1650 cm^{-1} of C=N groups.

3.1. The liquid crystalline properties

The transition temperatures and mesophase type were studied using hot-stage polarizing optical microscopy and DSC. The phase transition temperatures are summarized in **Table 1**. Microscopy examinations were used to determine the mesophase's texture using the categorization systems (25,26). At 275 ºC, all the compounds [V]n displayed enantiotropic dimorphism in the smectic A phase in addition to the nematic phase, as shown in **Figures 1a** and **1b** for compound [V]2 smectic A phase and compound [V]3 droplets nematic phase, respectively, **Figure 1c** for compound [V]6 and **Figures 1d** for compound [V]7. A graph of the transition temperature vs the number of carbon atoms (n) in the series [V]n alkoxy chain may be seen in **Figure 2**. In addition to the nematic-isotropic transition for compounds [V]1-7, compounds [V]1-8 demonstrated the odd-even effect of the crystal-smectic A and smectic A-nematic transitions. The DSC thermogram for compounds [V]2 and [V]7 is shown in **Figures 3** and **4**, respectively.

Table 1. Phase transition temperatures (ºC) of compounds $[V]_n$.

Compound No.	Transition phase
V_1	$\mathrm{Cr} \xrightleftharpoons{80} \mathrm{SmA} \xrightleftharpoons{160} \mathrm{N} \xrightleftharpoons{270} \mathrm{I}$
V_2	$\mathrm{Cr} \xrightarrow{94} \mathrm{Cr}$ $\mathrm{Cr} \xrightleftharpoons[185]{170} \mathrm{Sm\ A} \xrightleftharpoons[217]{247} \mathrm{N} \xrightleftharpoons{285} \mathrm{I}$
V_3	$\mathrm{Cr} \xrightleftharpoons{90} \mathrm{Sm\ A} \xrightleftharpoons{150} \mathrm{N} \xrightleftharpoons{280} \mathrm{I}$
V_4	$\mathrm{Cr} \xrightleftharpoons{100} \mathrm{Sm\ A} \xrightleftharpoons{180} \mathrm{N} \xrightleftharpoons{300} \mathrm{I}$
V_5	$\mathrm{Cr} \xrightleftharpoons{65} \mathrm{Sm\ A} \xrightleftharpoons{120} \mathrm{N} \xrightleftharpoons{240} \mathrm{I}$
V_6	$\mathrm{Cr} \xrightleftharpoons{85} \mathrm{Sm\ A} \xrightleftharpoons{190} \mathrm{N} \xrightleftharpoons{305} \mathrm{I}$
V_7	$\mathrm{Cr} \xrightarrow{87} \mathrm{Cr}$ $\mathrm{Cr} \xrightleftharpoons[191]{103} \mathrm{Sm\ A} \xrightleftharpoons[221]{145} \mathrm{N} \xrightleftharpoons{301} \mathrm{I}$
V_8	$\mathrm{Cr} \xrightleftharpoons{95} \mathrm{Sm\ A} \xrightleftharpoons{140} \mathrm{N} \xrightleftharpoons{210} \mathrm{I}$

Cr, Crystalline Phases; SMA, smectic A phase; N, nematic phase and I, isotropic liquid.

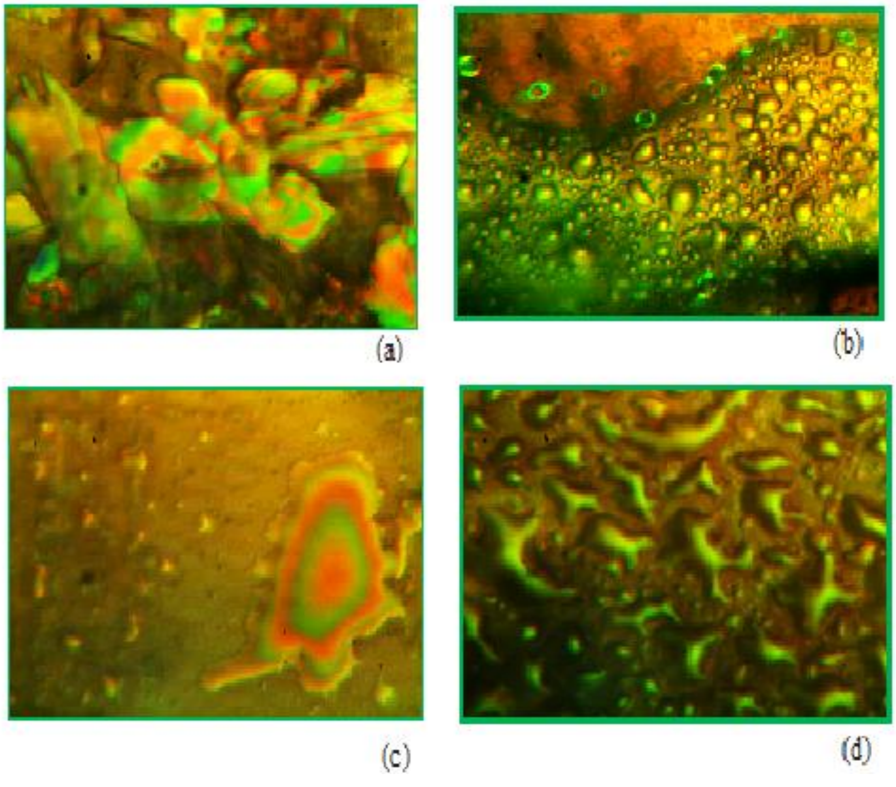

Figure 1. Cross polarizing optical textures of (a) smectic A phase for compound $[V]_2$ at 220 °C (b) droplets nematic phase for compound $[V]_3$ at 275 ºC (c) nematic phase for compound $[V]_6$ at 300 °C (d) nematic phase for compound $[V]_7$ at 295 ºC.

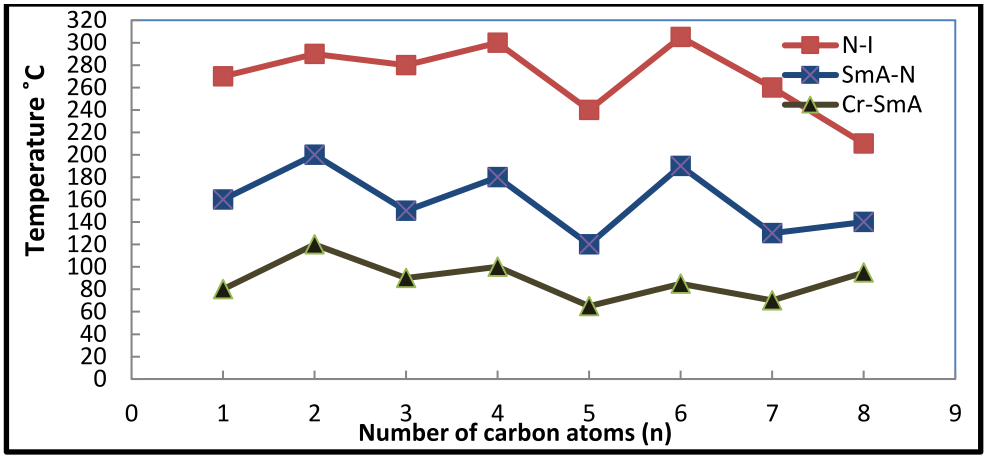

Figure 2. A graph of the transition temperature against the number of carbon atoms (n) in the [V]n alkoxy chain series.

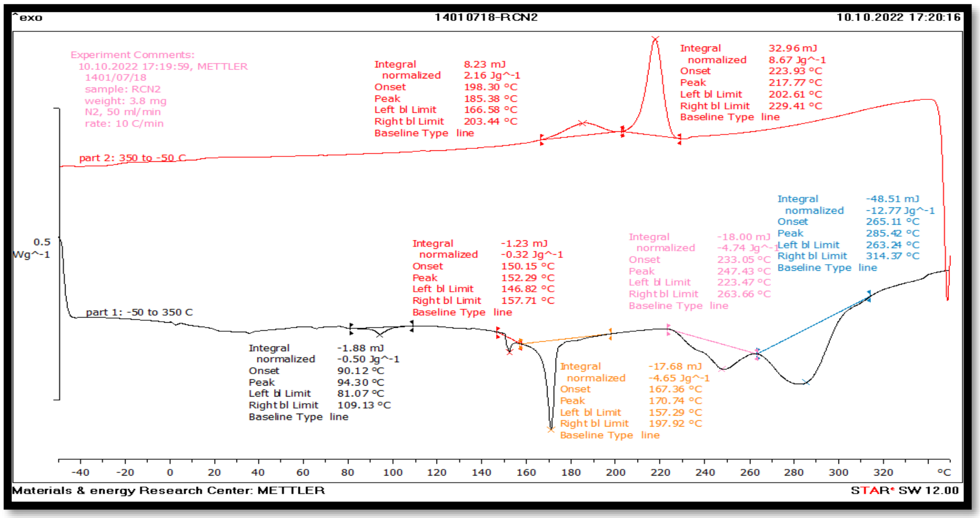

Figure 3. The DSC thermogram for compound [V]2.

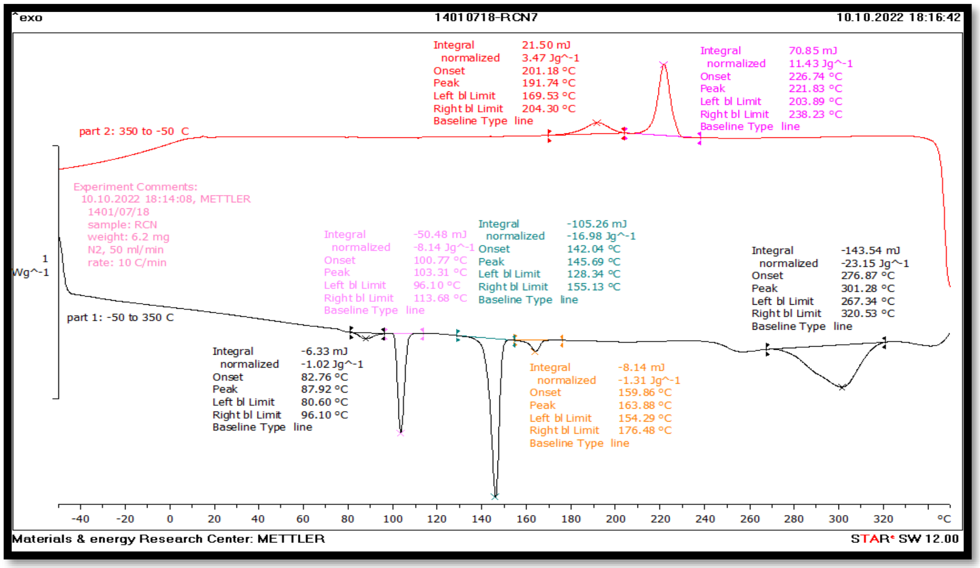

Figure 4. The DSC thermogram for compound [V]7.

The mesomorphic behavior of any intended liquid crystalline molecular architecture is typically governed by the kind of linking spacers, the size of the terminal chains, and the attached substituents (27, 28). The formation of a supramolecular hydrogen bond between the derivatives [V]1–8 in **Figure 5** lengthens the rigid-rod core of Schiff bases-based liquid crystals, significantly altering its properties and inducing the liquid crystalline nature of the interacting compounds (29,30). As a result, all of the Schiff-based compounds [V]1–8 displayed smectic dimorphism. A stage was other than the nematic phase.

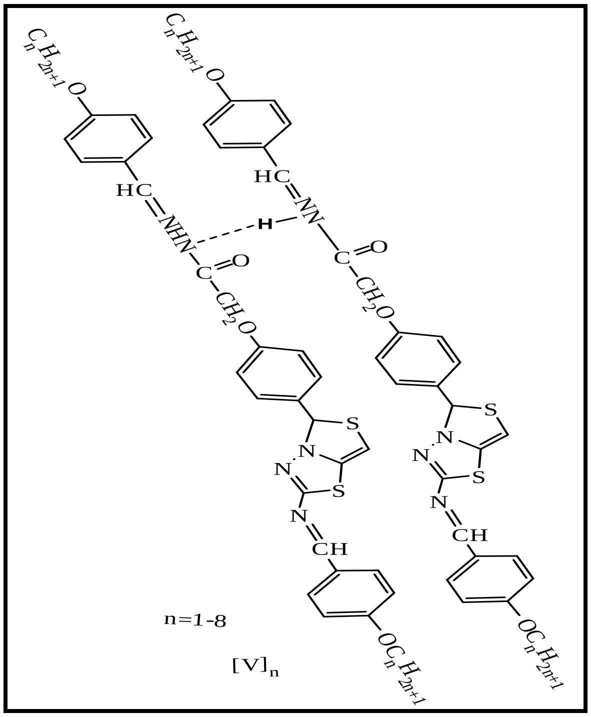

Figure 5. Compound [V]n forms hydrogen bonds.

4. Conclusion

The design and synthesis of novel thermotropic Schiff base liquid crystalline compounds, including 5*H*-thiazolo[3,4-b],[1,3,4] thiadiazole joined with an alkoxy group as the terminal chain length, were successfully synthesized and characterized in the study. Structural characterization was confirmed using FTIR and ^{1}H-NMR. The liquid crystal properties of these compounds were determined using POM, and their transitions were further confirmed using DSC. It was discovered that the mesophase type of H-bonding and the heterocyclic ring and terminal substituted effect. These compounds displayed liquid crystalline characteristics with a smectic A phase built on nematic mesophases.

Acknowledgment

This work was partially supported by the Department of Chemistry/ College of Education for Pure Science (Ibn Al- Haitham)/ University of Baghdad.

Conflict of Interest

The authors declare that they have no conflicts of interest.

Funding

No financial support was found.

Ethical Clearance

The Committee of the University of Baghdad/ College of Education for Pure Science (Ibn Al-Haitham) approved this study.

References

1. Knoerzer K, Regier M, Schubert H. Measuring temperature distributions during microwave processing. In: The microwave processing of foods. Woodhead Publishing; 2017, p. 327-349. https://doi.org/10.1016/B978-0-08-100528-6.00015-2.
2. Hu G, Qian W, Chang J, Yang Z, Wu X, Zhang K, Zhang B, Lu H, Kelly SM. Liquid crystalline materials containing pyrimidine rings. Liq Cryst. 2024; 51(10):1-34. https://doi.org/10.1080/02678292.2024.2361294.
3. Alamro FS, Gomha SM, Shaban M, Altowyan AS, Abolibda TZ, Ahmed HA. Optical investigations and photoactive solar energy applications of new synthesized Schiff base liquid crystal derivatives. Sci Reports. 2021; 11(1):15046. https://doi.org/10.1038/s41598-021-94533-6.
4. Gomha SM, Ahmed HA, Shaban M, Abolibda TZ, Khushaim MS, Alharbi KA. Synthesis, optical characterizations and solar energy applications of new Schiff base materials. Materials. 2021; 14(13): 3718. https://doi.org/10.3390/ma14133718.
5. Al-Mutabagani LA, Alshabanah LA, Gomha SM, Abolibda TZ, Shaban M, Ahmed HA. Synthesis and mesomorphic and electrical investigations of new furan liquid crystal derivatives. Front Chem. 2021; 9: 711862. https://doi.org/10.3389/fchem.2021.711862.
6. Park SH, Iwabata K, Sridhar U, Tsuei M, Singh K, Kim YK, Thayumanavan S, Abbott NL. A new strategy for reporting specific protein binding events at aqueous–liquid crystal interfaces in the presence of non-specific proteins. ACS Appl Mater Interfaces. 2019; 12(7):7869-7878. https://doi.org/10.1021/acsami.9b16867.
7. Michael T, Shivrayan M, Kim YK, Thayumanavan S, Abbott NL. Optical "blinking" triggered by collisions of single supramolecular assemblies of amphiphilic molecules with interfaces of liquid crystals. JACS. 2020; 142(13):6139-6148. https://doi.org/10.1021/jacs.9b13360.
8. Kim Y-K, Raghupathi KR, Pendery JS, Khomeini P, Sridhar U, De Pablo JJ, Thayumanavan S, Abbott NL. Oligomers as triggers for responsive liquid crystals. Langmuir. 2018; 34(34):10092-10101. https://doi.org/10.1021/acs.langmuir.8b01944.
9. Kim Y-K, Noh J, Nayani K, Abbott NL. Soft matter from liquid crystals. Soft Matter. 2019; 15(35): 6913-6929. https://doi.org/10.1039/C9SM01424A.
10. Nayani K, Yang Y, Yu H, Jani P, Mavrikakis M, Abbott. Areas of opportunity related to design of chemical and biological sensors based on liquid crystals. Liq Cryst Today. 2020; 29(2):24-35 https://doi.org/10.1080/1358314X.2020.1819624.
11. Parra M, Hidalgo P, Alderete J. New supramolecular liquid crystals induced by hydrogen bonding between pyridyl-1, 2, 4-oxadiazole derivatives and 2, 5-thiophene dicarboxylic acid. Liq Cryst. 2005; 32(4):449-455. https://doi.org/10.1080/02678290500075142.
12. Hofer S, Bodlos W, Novák J, Sanzone A, Beverina L, Resel R. Molecular packing analysis of the crystal smectic E phase of a benzothieno-benzothiophene derivative by a combined experimental/ computational approach. Liq Cryst. 2021; 48(13):1888-1896. https://doi.org/10.1080/02678292.2021.1907626.
13. Yang Y, Hao H, Zhao H. Synthesis and liquid crystal properties of benzoates containing 1, 2, 3-triazole. MCLC. 2022; 742(1):1-9. https://doi:10.1080/15421406.2022.2045115.
14. Chen R, Wang L, An Z, Chen X. Effect of π-conjugation units on the liquid crystal and photovoltaic performance of heterocyclic pyridine-based compounds. Liq Cryst. 2021; 48(15):2178-2187.https://doi.org/10.1080/02678292.2021.1934743.

15. Foo KL, Ha ST, Yeap G-Y, Lin HC. Mesomorphic behaviors of a series of heterocyclic benzothiazole-imine-ester-based liquid crystals. Phase Transit. 2019; 92(1):87-99. https://doi.org/10.1080/01411594.2018.1552272.
16. Foo K-L, Ha S-T, Yeap G-Y. Synthesis and phase transition behavior of calamitic liquid crystals containing heterocyclic core and lateral ethoxy substituent. Phase Transit. 2022; 95(2):178-192. https://doi.org/10.1080/01411594.2021.2023745.
17. Chang X-Y, Zhong W-Y, Han J. Synthesis, mesomorphic and fluorescent properties of stilbene-containing 1, 3, 4-oxadiazole compounds. Liq Cryst. 2023; 50(11-12):1709-1714. https://doi.org/10.1080/02678292.2023.2203104
18. Foo KL, Ha ST, Yeap GY, Lin HC. Synthesis and mesomorphic behaviors of a series of heterocyclic pyridine-imine-ester based liquid crystals. Phase Transit. 2019; 92(10):916-930. https://doi.org/10.1080/01411594.2019.1659265.
19. Shaalan Naser, Muwafaq SS. The synthesis, characterization and biological activity of some metal ions complexes with schiff's bases derived from reaction of 3-hydrazone-1, 3-dihydro-indole-2-one with 2-pyridine carboxaldehyde. IHJPAS. 2025; 38(1):279-292. https://doi.org/10.30526/38.1.3612.
20. Khalaf WY, Raheem LA, Youssef RS. Synthesis, identification, and biological evaluation of new coumarin-pyrazoline derivatives as anti-oxidant agents. Baghdad Sci J. 2025; 22(1):16-35. https://doi.org/10.21123/bsj.2024.8978.
21. Al-Mola IM, Al-Sabawi AH. Synthesis of some new hydrazide-hydrazone and heterocyclic compounds thiophene, imine, coumarin and pyrazole derivatives. Baghdad Sci J. 2024; 22(2):419-427. https://doi.org/10.21123/bsj.2024.9395.
22. Jabar MA, Karam NH. Synthesis and characterization of azo liquid crystal compounds based on 5H-Thiazolo [3, 4-b][1, 3, 4] thiadiazole unit. Revis Bionatura. 2022; 7(2):17. https://doi.org/10.21931/RB/2022.07.02.17.
23. Agili F. Novel hydrazide hydrazone derivatives as antimicrobial agents: design, synthesis, and molecular dynamics. Processes. 2024; 12(6):1055. https://doi.org/10.3390/pr12061055.
24. Younus MA, Hadi DJ. Synthesis, characterization and anticancer activity of poly acetal/pvp ag, au nanocomposite in treatment of lung cancer cell line. IHJPAS. 2025; 38(1):263-278. https://doi.org/10.30526/38.1.3607.
25. Dierking I. Textures of liquid crystals. John Wiley & Sons; 2003. https://doi.org/10.1002/3527602054.
26. 26. Goodby JW. Introduction to defect textures in liquid crystals. In: Handbook of visual display technology. Springer, 2016, p. 1897-1924. https://doi.org/10.1007/978-3-540-79567-4_82.
27. Omar AZ, Alazmi ML, Alsubaie MS, Hamed EA, Ahmed HA, El-Atawy MA. Synthesis of new liquid-crystalline compounds based on terminal benzyloxy group: Characterization, DFT and mesomorphic properties. Molecules. 2023; 28(9):3804. https://doi.org/10.3390/molecules28093804.
28. Alhaddad OA, Khushaim MS, Gogh SM, Ahmed HA, Naoum MM. Mesophase behavior of four ring ester/azomethine/ester liquid crystals in pure and mixed states. Liq Cryst. 2022; 49(10):1395-1402. https://doi.org/10.1080/02678292.2022.2037768.
29. Alaasar M, Tschierske C. Nematic phases driven by hydrogen-bonding in liquid crystalline nonsymmetric dimers. Liq Cryst. 2019; 46(1):124-130. https://doi.org/10.1080/02678292.2018.1476740.
30. Cheng X-H, Gao H-F. Hydrogen bonding for supramolecular liquid crystals. In book: Hydrogen bonded supramolecular materials. 2015, p.133-183. https://doi.org/10.1007/978-3-662-45780-1_5.